Supporting information

Cerium Hexacyanocobaltate: A Lanthanide-Compliant Prussian Blue Analog for Li-Ion Storage

Kaiqiang Zhang,[†,§] Tae Hyung Lee,[†] Joo Hwan Cha,[‡] Rajender S. Varma,[*,‖] Ji-Won Choi,[*,§] Ho Won Jang,[*,†] and Mohammadreza Shokouhimehr[*,†]

[†]Department of Materials Science and Engineering, Research Institute of Advanced Materials, Seoul National University, Seoul 08826, Republic of Korea

[‡]Small & Medium Enterprises Support Center, Korea Institute of Science and Technology (KIST), Seoul 02792, Republic of Korea

[§]Electronic Materials Center, Korea Institute of Science and Technology (KIST), Seoul 136-791, Republic of Korea

[‖]Regional Centre of Advanced Technologies and Materials, Faculty of Science, Palacky University in Olomouc, Šlechtitelů 27, 783 71 Olomouc, Czech Republic

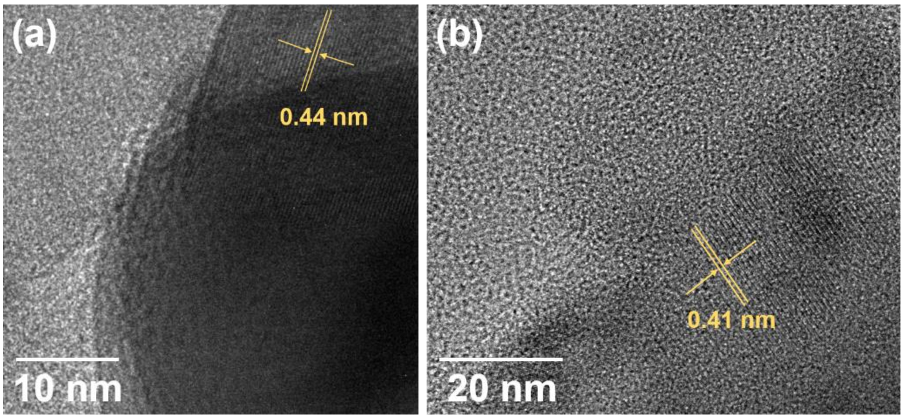

Figure S1. HRTEM images of the synthesized (a) FeHCCo and (b) CeHCCo NPs.

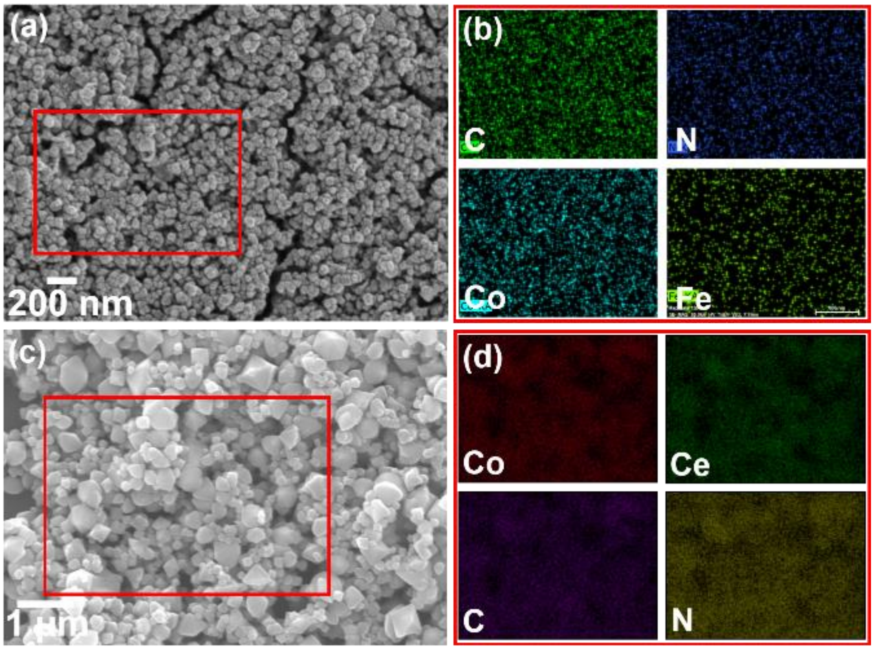

Figure S2. (a, c) SEM image and (b, d) EDS mapping of the synthesized FeHCCo (top) and CeHCCo (bottom) NPs.

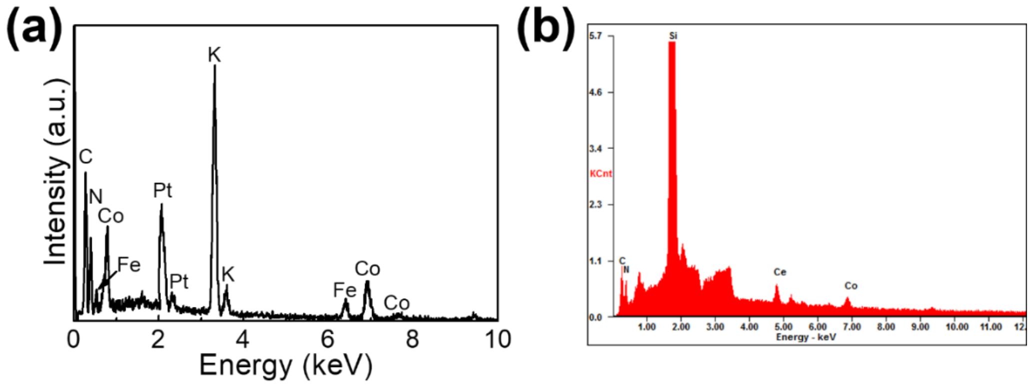

Figure S3. Qualitative elemental analysis by EDX mapping for the as-prepared (a) FeHCCo and (b) CeHCCo.

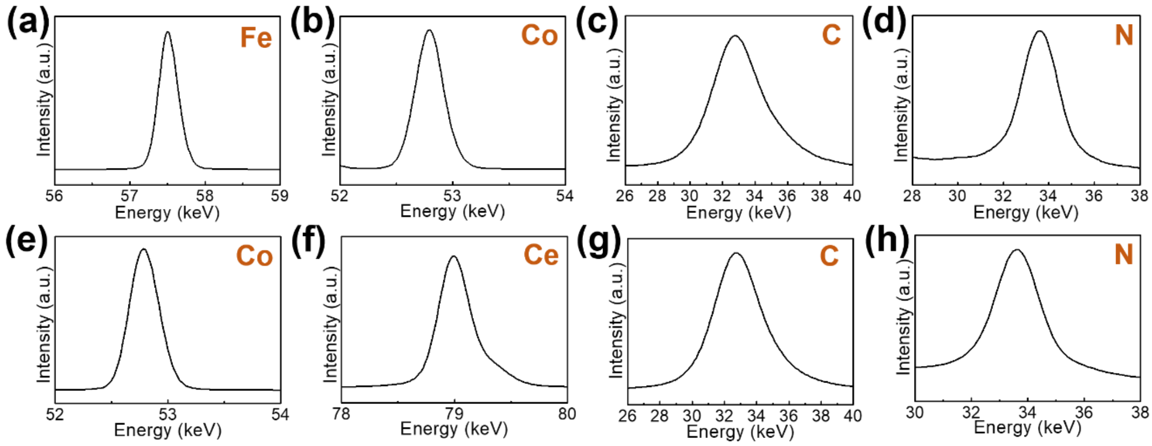

Figure S4. Qualitative elemental analysis by XRF mapping for the as-prepared (a−d) FeHCCo and (e−h) CeHCCo.

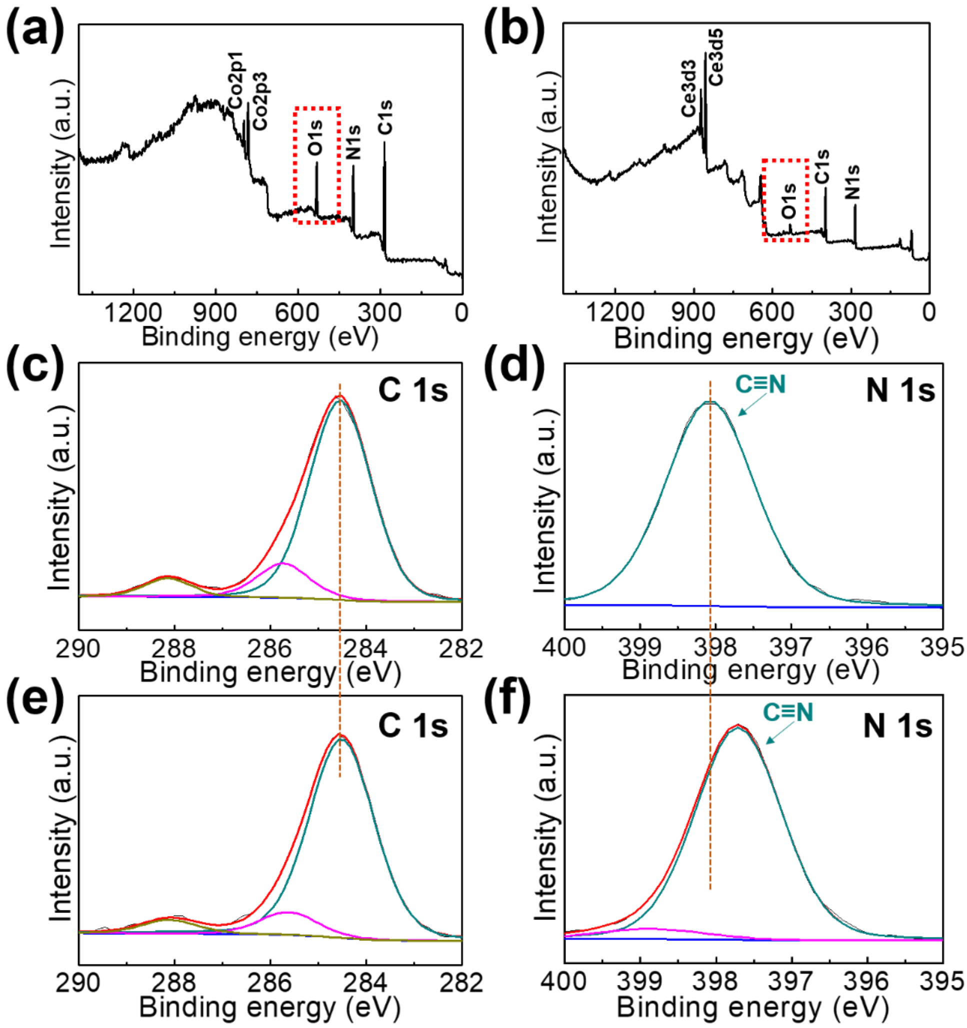

Figure S5. Wide survey of XPS for as-prepared (a) FeHCCo and (b) CeHCCo. Deconvoluted XPS spectra of (c) C 1s and (d) N 1s for FeHCCo and deconvoluted XPS spectra of (e) C 1s and (f) N 1s for CeHCCo.

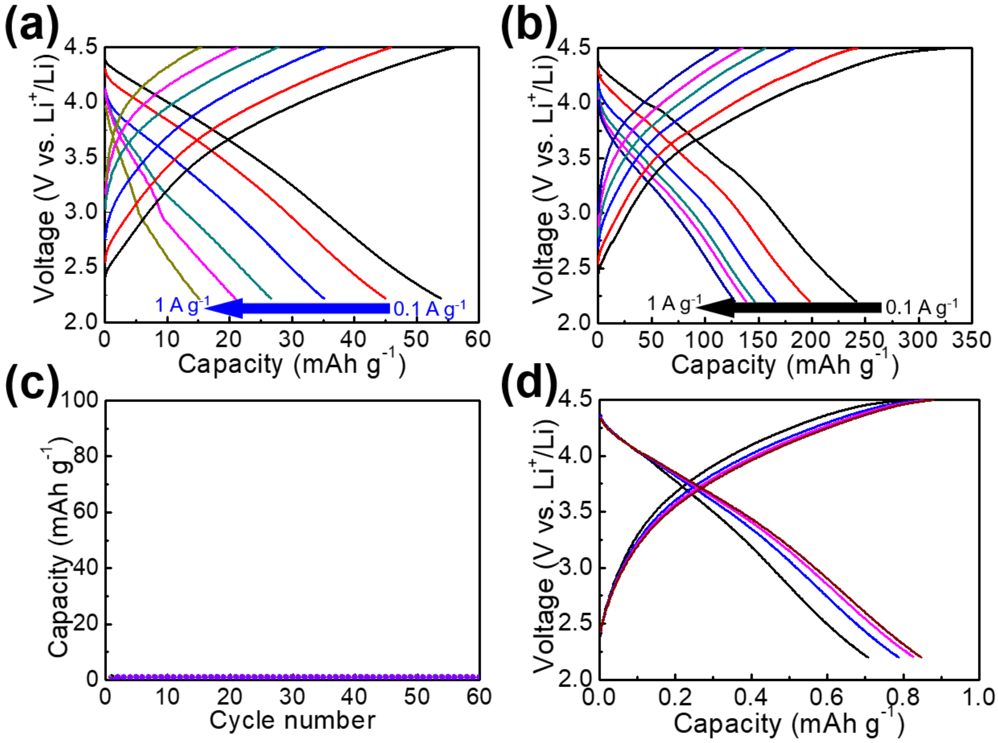

Figure S6. Representative charge/discharge curves for (a) FeHCCo and (b) CeHCCo. (c) Charge/discharge cycling measurement of graphite paper current collector. (d) Representative charge/discharge curves for graphite current collector.

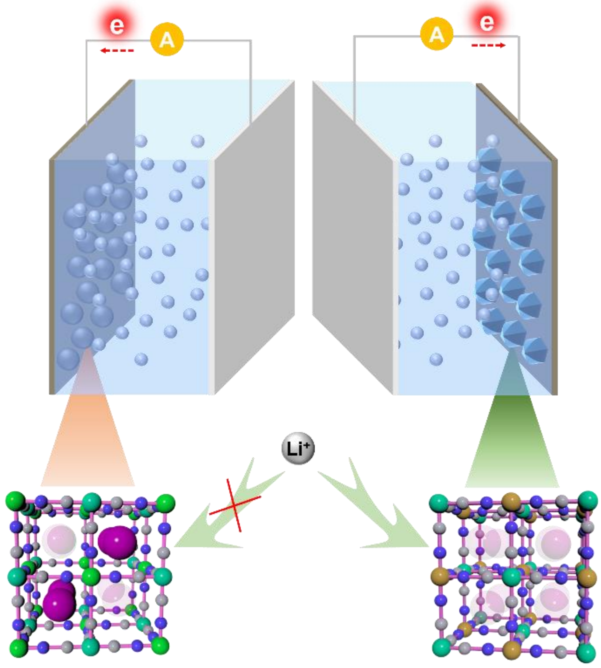

Figure S7. Schematic illustration of the discharge process of FeHCCo (left) and CeHCCo (right), where the encapsulated K^+ is expected to hinder the intercalation of Li^+.

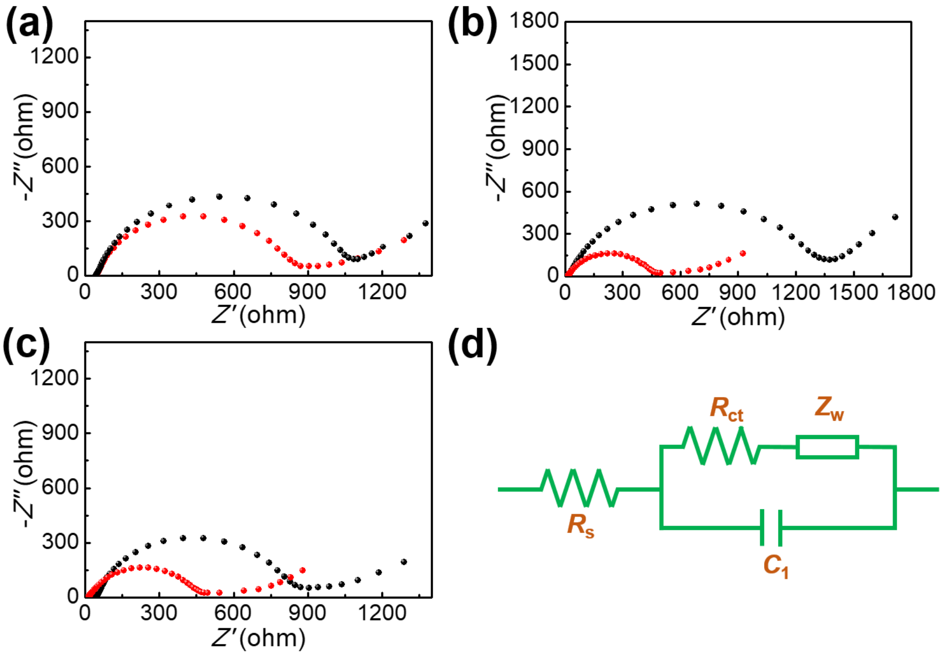

Figure S8. EIS spectra of (a) FeHCCo: fresh electrode (black dots) and after the first 5 cycle charge/discharge (red dots); (b) CeHCCo: fresh electrode (black dots) and after the first 5 cycle charge/discharge (red dots); (c): after the first 5 cycle charge/discharge of FeHCCo (black dots) and CeHCCo (red dots). (d) The corresponding equivalent circuit.

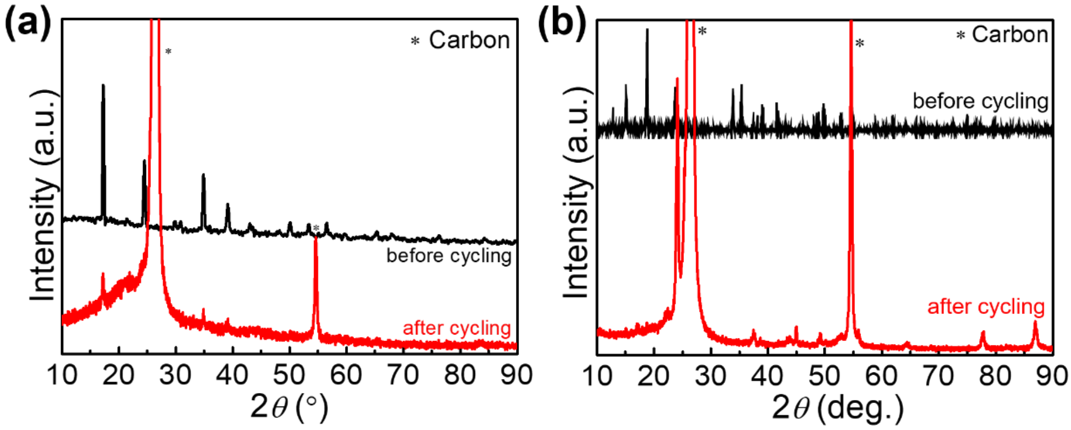

Figure S9. XRD spectra of (a) FeHCCo and (b) CeHCCo before and after charge/discharge cycling measurements. The carbon peaks originate from the graphite support.

Table S1. Quantitative elemental characterization for the as-prepared FeHCCo and CeHCCo.

Element	Wt. (%)	
	FeHCCo	CeHCCo
K	5	0.2
Fe	12	—
Ce	—	45
Co	9	19

Table S2. Quantitative elemental characterization for the as-prepared FeHCCo and CeHCCo by ICP.

Element	Amount (mg/L)	
	FeHCCo	CeHCCo
K	259	43
Fe	616	—
Ce	—	229
Co	241	241

Table S3. A comparison in capacity of the CeHCCo product and other reported Prussian blue analogs.

Entry	Material	Preserved capacity (mAh g^{-1})	Current density (mA g^{-1})	Cycling number	Reference
1	$K_{0.01}Ce[Co(CN)_6]_{0.99}$	177	100	100	This work
2	$Na_{1.32}Mn[Fe(CN)_6]_{0.83}$	~125	56	100	1
3	$Co_3[Fe(CN)_6]_2$	325	100	30	2
4	$Mn_3[Co(CN)_6]_2$	35.3	50	100	3
5	$Cu_{(0.5)}Mn_{(0.5)}$hexacyanoferrate	70	30	50	4
6	KFeHCF	104	100	70	5
7	NiFe-PBA	60	30	50	6
8	$KNi[Fe(CN)_6]$	52	12	50	7
9	$FeFe(CN)_6$	138	25	70	8

10	$Ti_{0.75}Fe_{0.25}[Fe(CN)_6]_{0.96}$	127	350	100	9
11	$Mn[Fe(CN)_6]_{0.6667}$	~540	100	20	10
12	$CeHCFe^{II}$	~50	100	70	11
13	$Fe^{III}HCCo$	~135	100	40	12

References:

(1) Matsuda, T.; Moritomo, Y. Thin film electrode of Prussian blue analogue for Li-ion battery. *Appl. Phys. Express* **2011**, *4*, 047101.

(2) Shokouhimehr, M.; Yu, S. H.; Lee, D. C.; Ling, D.; Hyeon, T.; Sung, Y.-E. Metal hexacyanoferrate nanoparticles as electrode materials for lithium ion batteries. *Nanosci. Nanotech. Let.* **2013**, *5*, 770–774.

(3) Nie, P.; Shen, L.; Luo, H.; Ding, B.; Xu, G.; Wang, J.; Zhang, X. Prussian blue analogues: a new class of anode materials for lithium ion batteries. *J. Mater. Chem. A* **2014**, *2*, 5852–5857.

(4) Okubo, M.; Honma, I. Ternary metal Prussian blue analogue nanoparticles as cathode materials for Li-ion batteries. *Dalton T.* **2013**, *42*, 15881–15884.

(5) Yu, S. H.; Shokouhimehr, M.; Hyeon, T.; Sung, Y. E. Iron hexacyanoferrate nanoparticles as cathode materials for lithium and sodium rechargeable batteries. *ECS Electrochem. Lett.* **2013**, *2*, A39–A41.

(6) Li, C. H.; Nanba, Y.; Asakura, D.; Okubo, M.; Talham, D. R. Li-ion and Na-ion insertion into size-controlled nickel hexacyanoferrate nanoparticles. *RSC Adv.* **2014**, *4*, 24955–24961.

(7) Omarova, M.; Koishybay, A.; Yesibolati, N.; Mentbayeva, A.; Umirov, N.; Ismailov, K.; Adair, D.; Babaa, M.-R.; Kurmanbayeva, I.; Bakenov, Z. Nickel hexacyanoferrate nanoparticles as a low cost cathode material for lithium-ion batteries. *Electrochim. Acta* **2015**, *184*, 58–63.

(8) Shen, L.; Wang, Z.; Chen, L. Prussian blues as a cathode material for lithium ion batteries. *Chem.-Eur. J.* **2014**, *20*, 12559–12562.

(9) Sun, X.; Ji, X.-Y.; Zhou, Y.-T.; Shao, Y.; Zang, Y.; Wen, Z.-Y.; Chen, C.-H. A new gridding cyanoferrate anode material for lithium and sodium ion batteries:

$Ti_{0.75}Fe_{0.25}[Fe(CN)_6]_{0.96}\cdot 1.9H_2O$ with excellent electrochemical properties. *J. Power Sources* **2016**, *314*, 35–38.

(10) Xiong, P.; Zeng, G.; Zeng, L.; Wei, M. Prussian blue analogues $Mn[Fe(CN)_6]_{0.6667}\cdot nH_2O$ cubes as an anode material for lithium-ion batteries. *Dalton T.* **2015**, *44*, 16746–16751.

(11) Peng, J.; Li, C.; Yin, J.; Wang, J.; Yu, Y.; Shen, Y.; Fang, J.; Chen, A.; Xu, Y.; Rehman, R.; Fang, C.; Miao, L.; Jiang, R.; Li, Q.; Han, J.; Huang, Y. Novel cerium hexacyanoferrate (II) as cathode material for sodium-ion batteries. *ACS Appl. Energy Mater.* **2018**, *2*, 187–191.

(12) Zhang, K.; Varma, R. S.; Jang, H. W.; Choi, J. W.; Shokouhimehr, M. Iron hexacyanocobaltate metal-organic framework: highly reversible and stationary electrode material with rich borders for lithium-ion batteries. *J. Alloy Compd.* **2019**, *791*, 911–917.